Biochimica et Biophysica Acta 1777 (2008) 1518–1527

Contents lists available at ScienceDirect

Biochimica et Biophysica Acta

journal homepage: www.elsevier.com/locate/bbabio

Intrinsic uncoupling in the ATP synthase of *Escherichia coli*

Manuela D'Alessandro [a,b], Paola Turina [a,*], B. Andrea Melandri [a]

[a] *Department of Biology, Laboratory of Biochemistry and Biophysics, University of Bologna, Via Irnerio 42, 40126 Bologna, Italy*
[b] *Department of Biochemistry, Schulich School of Medicine and Dentistry, Laboratory of Biochemistry and Molecular Biology, University of Western Ontario, London, Ontario N6A 5C1, Canada*

ARTICLE INFO

Article history:
Received 3 July 2008
Received in revised form 23 September 2008
Accepted 23 September 2008
Available online 8 October 2008

Keywords:
E. coli
ATP synthase
Uncoupling
H^+/ATP
Stoichiometry
Pi

ABSTRACT

The ATP hydrolysis activity and proton pumping of the ATP synthase of *Escherichia coli* in isolated native membranes have been measured and compared as a function of ADP and Pi concentration. The ATP hydrolysis activity was inhibited by Pi with an half-maximal effect at 140 μM, which increased progressively up in the millimolar range when the ADP concentration was progressively decreased by increasing amounts of an ADP trap. In addition, the relative extent of this inhibition decreased with decreasing ADP. The half-maximal inhibition by ADP was found in the submicromolar range, and the extent of inhibition was enhanced by the presence of Pi. The parallel measurement of ATP hydrolysis activity and proton pumping indicated that, while the rate of ATP hydrolysis was decreased as a function of either ligand, the rate of proton pumping increased. The latter showed a biphasic response to the concentration of Pi, in which an inhibition followed the initial stimulation. Similarly as previously found for the ATP synthase from *Rhodobacter caspulatus* [P. Turina, D. Giovannini, F. Gubellini, B.A. Melandri, Physiological ligands ADP and Pi modulate the degree of intrinsic coupling in the ATP synthase of the photosynthetic bacterium *Rhodobacter capsulatus*, Biochemistry 43 (2004) 11126–11134], these data indicate that the *E. coli* ATP synthase can operate at different degrees of energetic coupling between hydrolysis and proton transport, which are modulated by ADP and Pi.

1. Introduction

F_OF_1-ATPases or ATP synthases can be found in bacteria, mitochondria and chloroplasts [1–5]. These highly conserved enzymes catalyze ATP synthesis at the expense of a transmembrane electrochemical potential difference of protons (or Na^+ ions in some species) but can also work in the ATP hydrolysis direction, in this way building up a proton (or Na^+) electrochemical potential difference. They are composed of a membrane embedded hydrophobic sector, F_O, which is involved in proton translocation across the membrane, and in its simplest form contains 3 subunits in stoichiometry ab_2c_{10-15}, and of a hydrophilic extrinsic sector, F_1, which in its simplest form contains 5 subunits in stoichiometry $\alpha_3\beta_3\gamma\delta\varepsilon$ and the catalytic sites. In 1994 the first crystal structure of the bovine mitochondrial F_1 was reported by Abrahams et al. [6]. Following this achievement, further high resolution structural information for the soluble part has continued to appear, but a high resolution structure of the whole complex is still lacking.

As first proposed by Boyer [7,8], the catalytic nucleotide binding sites on the β-subunits operate in a cyclic way, which is accomplished by a rotatory movement of the γ-subunit within the $\alpha_3\beta_3$-subunit hexamer (reviewed in [3,9]). Beside the γ-subunit, the rotor is composed also of the ε-subunit in F_1 and of the *c*-subunit ring in F_O, and the rotary movement of the latter against the *a*-subunit is believed to be coupled to proton flow within F_O.

The stoichiometry of protons transported per ATP hydrolyzed or synthesized has usually been considered a fixed parameter under physiological conditions (but see [10] and references therein, [11,12]), although there have been several reports of conditions under which this stoichiometry was decreased, i.e. in mutated or chemically modified ATP synthases (see e.g. [13–18] and references therein), or when using non-physiological ligands such as Ca^{2+} in place of Mg^{2+} [19,20] or sulfite in place of Pi during hydrolysis [21]. Recently, we have found that the efficiency of proton transport in the ATP synthase of the photosynthetic bacterium *Rhodobacter capsulatus* can be decreased during physiological ATP hydrolysis, provided the concentrations of either Pi or ADP are kept sufficiently low [22].

One of the best known and most investigated ATP synthases, from a biochemical, functional and structural point of view, is that of *E. coli*. Therefore, it was of interest to check whether the same phenomenon could be found in this organism. It is already known that its ATP synthase, purified and reconstituted into liposomes, is inhibited in the

Abbreviations: EF_1F_O, ATP synthase of *E. coli*; EF_1, hydrophilic subcomplex of the ATP synthase of *E. coli*; Tricine, N-[2-Hydroxy-1,1-bis(hydroxymethyl)ethyl] glycine; PK, pyruvate kinase; Phenol Red, 4,4′-(3H-2,1-benzoxathiol-3-ylidene) bis-phenol, S,S-dioxide; $\Delta\psi$, bulk-to-bulk transmembrane electrical potential difference; LDH, lactate dehydrogenase; LDAO, lauryldimethylamine oxide; ACMA, 9-amino-6-chloro-2-methoxyacridine; $\Delta\tilde{\mu}H+$, transmembrane difference of electrochemical potential of protons; ΔpH, transmembrane difference of pH

* Corresponding author. Tel.: +39 051 2091322; fax: +39 051 242576.
E-mail address: paola.turina@unibo.it (P. Turina).
URL: http://www.biologia.unibo.it/ (P. Turina).

0005-2728/$ – see front matter © 2008 Elsevier B.V. All rights reserved.
doi:10.1016/j.bbabio.2008.09.011

hydrolysis direction by the binding of ADP and Pi, with apparent Kd's of 10 and 470 μM, respectively, and that the inhibited ATP hydrolysis activity is recovered if a protonmotive force is applied [23].

In the present work, our goal was to investigate whether the binding of ADP and Pi to the *E. coli* ATP synthase was not only inhibitory of hydrolysis but would also elicit the transition from a partially uncoupled to a fully coupled form of the enzyme. Our results show that regulatory phenomena of proton transport involving ADP and Pi binding are operative also in the ATP synthase of *E. coli*, although their features differ somewhat from those shown in *Rb caspulatus*. They open the way to mutational studies, easily performed in this bacterium, aimed at investigating the coupling mechanism in the ATP synthases. A preliminary account of these results has been presented in [24].

2. Materials and methods

2.1. Membrane preparation

Cells from the XL1Blue *E. coli* strain carrying the kanamycin resistance on the plasmid pNK1 (Stratagene) were grown on LB medium, and harvested at a late exponential phase. Membranes were isolated from cells essentially as described in [25]. Cells were resuspended with 5 ml/g wet weight of a buffer containing 10 mM Tricine/NaOH pH 7.5, 5 mM $MgCl_2$, 10% glycerol, 6 mM p-aminobenzamide and disrupted at 138 Mpa (20,000 p.s.i.) with a French-Press. Unbroken cells were removed by centrifugation at 16,000 rpm and the remaining supernatant was recentrifuged in a Beckman type 50.2 Ti rotor at 40,000 rpm for 90 min. The pellet was resuspended in a small volume of the same buffer, rapidly frozen as 50 μl aliquots in liquid nitrogen, and stored at −80 °C. Total protein concentration was measured by the Bradford method [26].

2.2. ATP hydrolysis

All reactions were carried out in sample holders thermostated at 26 °C. In the absence of pyruvate kinase (PK), ATP hydrolysis was measured by detecting the scalar protons released upon ATP hydrolysis with the colorimetric pH indicator Phenol Red. Membranes were suspended to 0.025 mg/ml in the following buffer: 1 mM Tricine, 50 mM KCl, 2.0 mM $MgCl_2$, NaOH to pH 8.0, and 1 μM valinomycin to minimize $\Delta\varphi$. Phenol Red was added to 100 μM. Prior to each measurement, the sample pH was adjusted to 8.0 with NaOH. The pH changes of the suspension were followed as a function of time by the absorbance changes at 625–587 nm, and were calibrated after about 200 s of reaction by 3 sequential addition of 15 μM HCl. The overall pH change of the suspension at the end of the measurements was never higher than 0.3 U. The calibration signals showed that the addition of 3 mM Pi in the poorly buffered assay medium caused a less than 2-fold increase of the buffering power. The changes of proton concentration were transformed to changes of ATP concentration as described [27]. At pH 8.0 an H^+/ATP ratio of 0.94 was used. When ATP hydrolysis was measured in parallel samples with the malachite green assay [28], the same rates were obtained within experimental error, indicating absence of significant artefacts in the Phenol Red assay. For measurements in the presence of PK (ADP trap), the reaction temperature and ATP hydrolysis mixtures were the same as used in the Phenol Red assay, including the low buffer concentration, except that 2 mM PEP, PK to variable amounts, 25 U/ml of lactate dehydrogenase (LDH), 0.15 mM NADH and 2 mM KCN were present and no Phenol Red was added. The PK was supplied from Sigma (P-9136) as a ion-free lyophilized powder. The ADP trap was thus coupled to NADH oxidation, and the absorbance changes at 340 nm were followed as a function of time. Again, control samples were set up in which ATP hydrolysis was measured with the malachite green assay in the presence of the ATP regenerating system, and the same rates were obtained within experimental error. In the absence of ATP, no significant NADH oxidation could be detected, and in control ACMA assays it was confirmed that 2 mM KCN were enough to completely inhibit the NADH-driven ACMA quenching, indicating a sufficient inhibition of the *E. coli* respiratory chain. DCCD inhibition was obtained by incubating the membranes for at least 30 min at a concentration of 2.5 mg/ml in the presence of 250 μM inhibitor; under such conditions the activity measured in the presence of 0.5% LDAO was not significantly affected, indicating that the observed inhibition did not involve the F_1 sector.

2.3. 9-Amino-6-chloro-2-methoxyacridine (ACMA) assay

The ACMA assays were carried out under experimental conditions as close as possible to those used for ATP hydrolysis measurements. The ACMA fluorescence emission was recorded as a function of time (RC=0.25 s) in a Jasco FP 500 spectrofluorometer (wavelength 412 and 482 nm for excitation and emission respectively) at 26 °C. For measurements in the absence of PK, the assay mixture was the same as used for Phenol Red assay, including the low buffer capacity, except that Phenol Red was omitted and 1.5 μM ACMA was added. When an ADP trap was present, the assay mixture was the same as used for measurements of ATP hydrolysis in the presence of PK, except that LDH, NADH and KCN were omitted. In control measurements it was shown that pyruvate up to 100 μM did not affect the quenching signals.

2.4. Measurement of pyruvate kinase activity

The activity of PK under the experimental conditions of the present work was measured at 26 °C. The buffer in the absence of any membranes was supplemented with 2 mM PEP, 2 mM ADP, 0.15 mM NADH, 25 U/ml LDH. The reaction was started in the spectrophotometer by addition of PK (nominally 0.03 U/ml) and the coupled NADH oxidation was recorded at 340 nm.

3. Results

In order to evaluate the relative coupling degree of the *E. coli* enzyme as a function of Pi and ADP, we carried out both hydrolysis and proton pumping measurements in parallel in the isolated membrane vesicles, taking special care in keeping constant all experimental conditions in each double series of measurements.

3.1. Effect of Pi on ATP hydrolysis and proton pumping

Inorganic phosphate has been reported to strongly inhibit the ATP hydrolysis of the isolated, reconstituted EF_1F_O [23] and of the isolated EF_1 [29,30], with apparent Kd's in the order of a few hundred micromolar.

Therefore, we first measured ATP hydrolysis as a function of Pi, to check whether this behavior could be reproduced in the isolated internal membranes. Fig. 1A shows the amount of hydrolyzed ATP as a function of time after addition at t=0 s of 25 μM ATP, in the presence of increasing Pi concentrations; valinomycin and 50 mM K^+ were also present, in order to have the same assay composition as used in the ACMA assay (see below). The rates of ATP hydrolysis at t=0 s and t=50 s were evaluated by fitting the spectrophotometric data (collected at a rate of 1/s) with a monoexponential function and taking the first derivatives at t=0 s and t=50 s respectively. These rates decreased at increasing Pi concentrations, confirming that Pi inhibited the hydrolysis activity also in the non-isolated enzyme. The DCCD-insensitive activity is also shown for comparison. At each Pi concentration, the hydrolysis rates decreased with time, an effect which can be attributed to decreasing ATP and/or accumulating ADP, since the same reactions carried out in the presence of an enzyme-coupled ATP regenerating system had a fully linear time-course (see below). By plotting the initial rates as a function of Pi (Fig. 1B, full

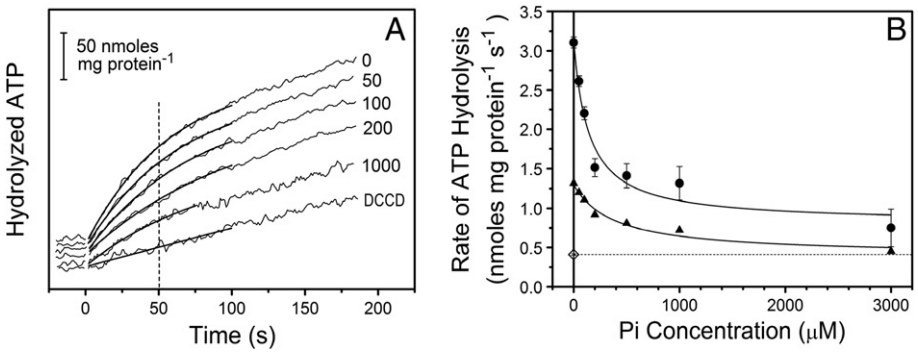

Fig. 1. ATP hydrolysis rate as a function of Pi concentration. The ATP hydrolysis assay was carried out with Phenol Red as a pH indicator for the release of scalar protons as described in the Materials and methods. (A) The ATP hydrolysis reaction was started at time t=0 s in the spectrophotometer by addition of 25 μM ATP and the absorbance (625–587 nm) was measured as a function of time. Absorbance values were converted to hydrolyzed ATP as described in the Materials and methods. Different Pi concentrations were added to each assay as indicated. For specifically inhibiting the ATP synthase activity, the reaction mixture was incubated in the presence of 250 μM DCCD for 30 min before starting the reaction. The experimental traces were best fitted by monoexponential functions (or linear in the case of DCCD) up to 100 s (75 s for Pi=1 mM). (B) Rates of ATP hydrolysis at t=0 s (●) and at t=50 s (▲) and DCCD-insensitive rate (◊) are from Panel A and additional measurements, and have been calculated from the fitting functions; the errors of the rates at t=0 s have been calculated from the errors associated with the amplitude and time constant of the monoexponentials. The curves through the ATP hydrolysis data points are the best fit to the data of the hyperbolic function $P_1 - P_2 \cdot x/(P_3 + x)$, with resulting best fit parameters $P_3 = 140 \pm 50$ μM (●) and $P_3 = 400 \pm 200$ μM (▲) respectively, corresponding to the apparent Kd values.

circles), an hyperbolic trend was obtained, with a best-fitting value of 140 μM for the apparent Kd. The rates at t=50 s are also plotted (full triangles), which can be similarly interpreted as having an hyperbolic trend.

The proton translocating activity of the ATP synthase was estimated using the fluorescent ΔpH-sensitive acridine dye ACMA. The fluorescence measurements were carried out under the same experimental conditions of the ATP hydrolysis measurements, except for the absence of Phenol Red and the presence of ACMA. Valinomycin and 50 mM K^+ were always present in order to minimize the electrical component of the protonmotive force, so that the $\Delta\tilde{\mu}_{H^+}$ consisted of ΔpH only.

Fig. 2A and B shows the ACMA fluorescence as a function of time in the presence of different added Pi concentrations. After starting the proton transport reaction by addition of 25 μM ATP at t=0 s, a rapid fluorescence quenching was observed in all cases, indicating a rapid acidification of the vesicles' interior, which settled to a steady state quenching level within 1–2 min, and could be reversed by the addition of nigericin. No significant fluorescence quenching was detected in samples pretreated with DCCD (not shown). Notably, this steady state level was increased in the presence of Pi concentrations up to 100 μM (Fig. 2A), while higher concentrations resulted in a progressive inhibition of proton pumping (Fig. 2B). A similar biphasic response to Pi could also be observed in the initial rates of fluorescence quenching

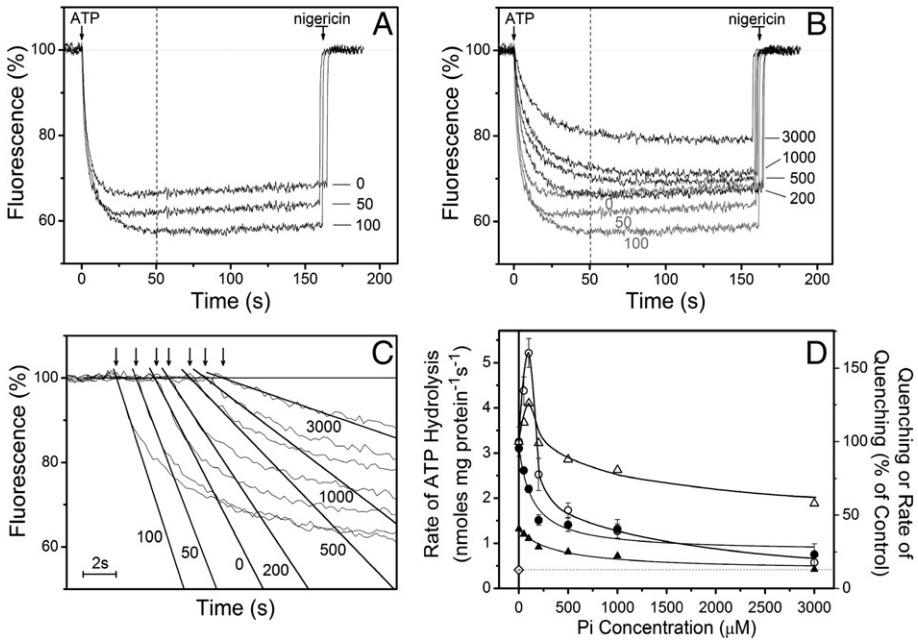

Fig. 2. ACMA fluorescence quenching as a function of Pi concentration. The ACMA assay was carried out as described in the Materials and methods. (A,B) The proton pumping reaction was started in the spectrofluorimeter cuvette by addition of 25 μM ATP at time t=0 s and the ACMA fluorescence was recorded as a function of time. Different Pi concentration were added to each assay as indicated. For each trace, addition of 2 μM nigericine recovered the 100% fluorescence level. The traces are reported in two panel for improved clarity (the traces obtained at Pi concentrations ≤100 μM (A) are reported in gray in (B) for comparison). (C) The traces in (B) are reported here on a shorter time scale and displaced along the time axis for showing the initial rates of quenching. The arrows indicate the time points of ATP addition, the numbers the Pi concentrations. The linear fits were calculated over 1 (0–500 μM Pi) or 2 (1–3 mM Pi) s of reaction (5 or 9 data points). (D) The percentage values of the initial rates of fluorescence quenching (○) and of fluorescence quenching at t=50 s (Δ) relative to controls (7.6% · s^{-1} and 33.8%, respectively) were determined from (B) and (C). The errors of the initial rates of quenching are the errors associated with the first-order coefficients of the linear regressions. The values of the initial rates of ATP hydrolysis (●) and of the rates at t=50 s (▲) are reported for comparison from Fig. 1B. The curves through the quenching data points were drawn by hand.

(Fig. 2C). In Fig. 2D both the steady state (at t = 50 s) and the initial rate values of fluorescence quenching were plotted as a function of added Pi (open symbols). In the same figure the hydrolysis rates from Fig. 1B (at t = 0 s and t = 50 s) are also reported for comparison (closed symbols). The plot highlights the different courses of both quenching curves, markedly biphasic (first activatory and then inhibitory), and of the two hydrolysis curves, monotonically inhibitory. Analogous experimental results had been preliminarily obtained using vesicles from the ATPase superproducer strain of *E. coli* AN1460, carrying a copy of the *unc* operon on the multicopy pAN45 plasmid (data not shown). The very fast fluorescence response of ACMA observed using these vesicles had prevented us, however, from performing an analysis in terms of initial rates.

In the case of a pumping enzyme which keeps the number of protons translocated per hydrolyzed ATP constant, a parallel behavior of hydrolysis and ACMA response is expected. In such a case, a higher initial rate of hydrolysis will be associated, at constant internal buffering capacity, with a higher rate of ACMA quenching. In fact, the ACMA quenching has been shown to be a monotonically increasing, though not linear, function of transmembrane ΔpH (see e.g. [31] for a theoretical model and [32–34] for an experimental calibration of the response of ACMA and other acridine dyes by means of acid-base transitions). Similarly, again in the case of a constant number of protons transported per hydrolyzed ATP, the steady state transmembrane ΔpH, and therefore the steady state fluorescence quenching, is expected to increase or decrease in parallel with the rate of ATP hydrolysis, provided the passive proton permeability coefficient of the membrane does not change. In fact, the higher the inward proton flux, the higher will be the ΔpH at which this active inward proton flux will be balanced by the passive outward proton flux (which at constant proton permeability coefficient is an increasing function of the ΔpH itself).

3.2. Evaluation of the ACMA response in the E. coli membrane system

The following measurements were carried out in order to confirm that also in our system the response of ACMA increased in parallel to increasing steady state ΔpH and initial rate.

The ACMA response was measured as a function of ATP concentration, and the results were indeed as expected, in that the steady state quenching increased in parallel with ATP (Fig. 3A, traces (a) through (e)), and so did the initial rate of quenching (Fig. 3B). These initial rates of quenching are plotted as a function of ATP concentration together with the initial rates of ATP hydrolysis (Fig. 3C), which were measured in parallel in the Phenol Red assay under the same experimental conditions. The increase in the rate of hydrolysis was almost linear in the measured range, consistent with a K_M value in the hundreds of μM range (K_M = 140 μM ATP was obtained in the isolated and reconstituted enzyme in [35]) and was closely paralleled by the initial rate of quenching, which had a less linear run, consistent with the non-linear response of ACMA to the transmembrane ΔpH [32–34]. During the recording of the trace at 5 μM ATP ((a) in Fig. 3A), the further addition of 50 μM ATP restored a steady state quenching value similar to the one of the 50 μM ATP trace (d), indicating that the slow regain of fluorescence in trace (a) was mainly due to substrate depletion. Addition of 50 μM NADH (both trace (a) and trace (e)) showed that the activation in parallel of a second source of proton translocation (respiratory chain) further increased the steady state quenching, consistent with a parallel increase of inward proton flux and consequently with a higher steady state ΔpH. Finally, it can be noted that in Fig. 3C the highest quenching rate values obtained as a

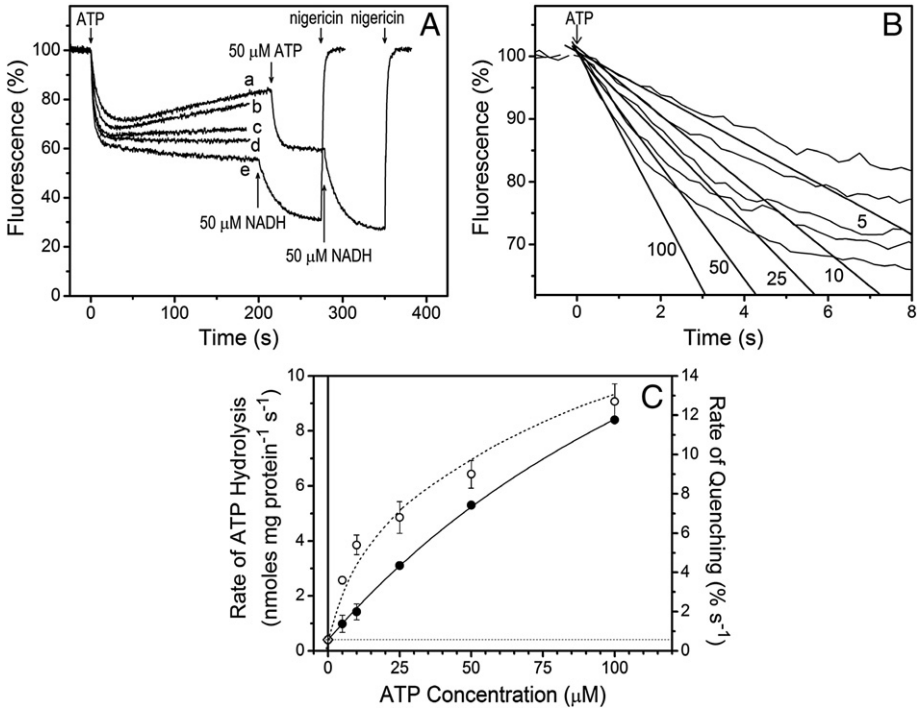

Fig. 3. ACMA fluorescence quenching as a function of ATP concentration. The ACMA assay was carried out as described in the legend of Fig. 2. The ATP concentrations were (a) 5 μM, (b) 10 μM, (c) 25 μM, (d) 50 μM, (e) 100 μM. For the trace at 5 μM ATP, a second addition of 50 μM ATP after about 200 s is indicated by an arrow. The further additions of 50 μM NADH for the traces at (5 + 50) μM and 100 μM ATP are indicated by arrows. (B) The traces from (A) are reported on a shorter time scale. The numbers indicate the ATP concentrations. The linear fits were calculated over 1 or 2 s of reaction (5 or 9 data points). (C) The values of the initial rates of fluorescence quenching (○) (from (B)) are reported as a function of ATP concentration. The errors of the initial rates of quenching are the errors associated with the first-order coefficients of the linear regressions. The values of the initial rates of ATP hydrolysis (●) and their errors were determined, similarly as described for Fig. 1, from monoexponential fitting of Phenol Red traces of ATP hydrolysis measurements carried out as a function of ATP concentration. The curve through the quenching data points was drawn by hand, the curve through the hydrolysis data points is a best fitting hyperbole with apparent K_M = 190 ± 20.

function of ATP concentration are in the same range as the highest rates obtained as a function of Pi (Fig. 2D), indicating that these latter were not significantly limited by lack of kinetic competence of ACMA. This kinetic competence is consistent with the data reported in [32,36], indicating that acridines respond to ΔpH changes within hundreds of milliseconds.

As mentioned, the interpretation of the increasing rates of ACMA quenching (data in Fig. 2) as corresponding to increasing rates of proton translocation mainly requires that the internal buffer capacity of the vesicles remains constant in the range of Pi concentration in which the phenomenon is observed. Assuming complete permeation of Pi through the membrane (which is an extreme assumption in view of its 1–2 charges at pH 8), it can be excluded that a few hundred μM Pi (with pK = 7.2) could significantly alter the buffer capacity of the inner bulk phase, which should be buffered by 1 mM Tricine (pK = 8.2), and even in this case, the buffering would determine a decrease of the initial rate, relative to the initial rate at Pi = 0, and not an increase. As to the decreasing phase of the Pi dependency of the quenching rate, it cannot be excluded that a small part of the observed decrease was due to Pi permeation to the vesicle inside, but a very similar decrease was observed also when the buffer contained 20 mM Tricine (not shown).

The interpretation that the increasing steady state of ACMA quenching, seen with increasing Pi (data in Fig. 2), corresponds to increasing rates of proton translocation also requires, as mentioned, that the proton permeability of the membrane is not changed by the changing concentration of Pi (e.g. through Pi binding to, and activation of, membrane channels). We checked for this possibility by measuring, as a function of Pi, the steady state quenching signal induced by 50 μM NADH, or, in order to include nucleotides as well, by repeating the same measurements in the presence of 20 μM ATP and 5 μM ADP in a DCCD inhibited sample (not shown). No significant change in the steady state quenching could be detected in either case.

We conclude that the interpretation of increasing initial quenching rates and increasing steady state quenching in the low Pi concentration range as being due to increasing proton translocation rates by the ATP synthase is warranted in our system. According to this interpretation, the binding of Pi at low concentration to ATP synthase increases its rate of proton translocation while decreasing its rate of ATP consumption. The only plausible explanation for this phenomenon that we can see is that Pi binding at low concentration increases the ratio of protons translocated per hydrolyzed ATP, or, in other words, that it increases the efficiency of proton translocation from a relatively inefficient state to a much more efficient one.

3.3. Effect of ADP depletion on the Pi inhibited ATP hydrolysis

The inhibition by saturating Pi of the ATP hydrolysis by the isolated and reconstituted *E. coli* ATP synthase has been shown to be strongly enhanced by the presence of ADP and, vice versa, the inhibition by saturating ADP was strongly enhanced by Pi [23].

We checked, therefore, whether the same phenomenon could be shown in the enzyme embedded in native membranes. Given the high Pi inhibition observed in the absence of added ADP, it was likely that ADP was already present in our system, either pre-bound to the synthase or present in sufficient amounts in the ATP solution. In order to deplete our system from ADP, we measured the rate of ATP hydrolysis with an enzyme-coupled ATP regenerating system (see Materials and methods), in which PK and PEP operated as an ADP trap, and LDH and NADH (in the presence of KCN for inhibiting the NADH-driven respiratory chain) coupled the ATPase reaction (through the PK and LDH reaction) to the absorbance changes at 340 nm. The steady state ADP concentration was modulated through the amount of added PK: different series of measurements as a function of Pi were carried out in the presence of increasing amounts of PK in the assay, i.e. at decreasing concentration of steady state ADP. At all Pi and PK concentrations, addition of 25 μM ATP started a decrease in the absorbance, i.e. ATP hydrolysis, which was linear over the whole measuring time (200 s), except for an initial fast phase of 1–2 s, which could be attributed to rapid phosphorylation of the ADP present as a contaminant in the ATP solution, since it could be observed also in the absence of membranes. The hydrolysis rates are plotted in Fig. 4 as a function of Pi concentration for all tested PK activities, together with the hydrolysis rates from Fig. 1B (full circles) obtained in the absence of PK. The curves through the data points are hyperbolic functions best-fitted to the data. An effect of PK on the inhibition by Pi is evident: at intermediate PK amounts (2, 10, and 55 U/ml) the apparent Kd's for Pi shift to progressively higher values (290, 520, and 1100 μM respectively) until, at the highest PK amount (110 U/ml), an inhibition by Pi is barely detectable. The asymptotic levels of inhibition were gradually decreased as well. Therefore the activating effect of the ADP trap is most evident at the highest Pi concentrations.

These results confirm and extend those first obtained in the isolated and reconstituted EF_1F_O [23], in showing that ADP bound to the enzyme is required for Pi to be able to inhibit ATP hydrolysis. Analogously, Pi is required for a stronger inhibition by ADP, although the inhibitory effect of ADP can be observed also in the absence of added Pi.

3.4. Effect of ADP depletion on proton pumping

We then measured the ATP-driven ACMA fluorescence quenching under the same experimental conditions of Fig. 4. The assay compositions were identical to those of Fig. 4 except that LDH, NADH and KCN were omitted and ACMA was present. In the fluorescence traces shown in Fig. 5, Pi was kept constant at 200 μM, and the amount of PK added to the assay was progressively increased from 0 to 110 U/ml. After addition of 25 μM ATP at t = 0 s, a fast rate of fluorescence quenching was observed in all cases, which declined with time. Such decline was most pronounced in the case of no added PK, showing that substrate depletion and ADP accumulation contributed to this decline. Noticeably, the overall quenching signal was significantly increased, relative to no addition, by the presence of 2 U/ml of PK, but such high quenching level was progressively decreased when increasing PK activities were added. A very similar trend could be observed in the initial rate of fluorescence quenching (Fig. 5B). The increase in both overall quenching signal and initial quenching rate at 2 U/ml PK was in agreement with the increase of the hydrolysis rate observed at 200 μM Pi at the corresponding level of PK (see Fig. 4). By

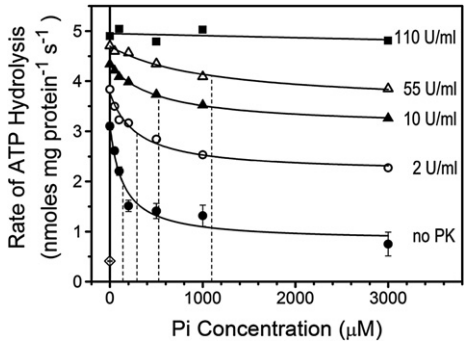

Fig. 4. ATP hydrolysis rate as a function of Pi concentration in the presence of increasing PK activity. ATP hydrolysis reactions as a function of Pi concentration were started in the presence of PK by adding 25 μM ATP and were measured as the disappearance in time of NADH absorbance in the presence of an enzyme-coupled ATP regenerating system, as described in the Materials and methods. Data points obtained in the absence of PK (●), or after inhibition by DCCD (◊) are reported from Fig. 1B for comparison. The ATP regenerating system contained increasing activities of PK as indicated. The curves through the data points at 0 (●), 2 (○), 10 (▲) and 55 U/ml (△) are the best fit to the data of the hyperbolic function $P_1 - P_2 \cdot x/(P_3 + x)$, with resulting best-fit parameters $P_3 = 140 \pm 50$, 290 ± 80, 520 ± 60 and 1100 ± 400 μM, respectively, as indicated by the dashed lines. The curve through the data points at 110 U/ml (■) is a linear fit.

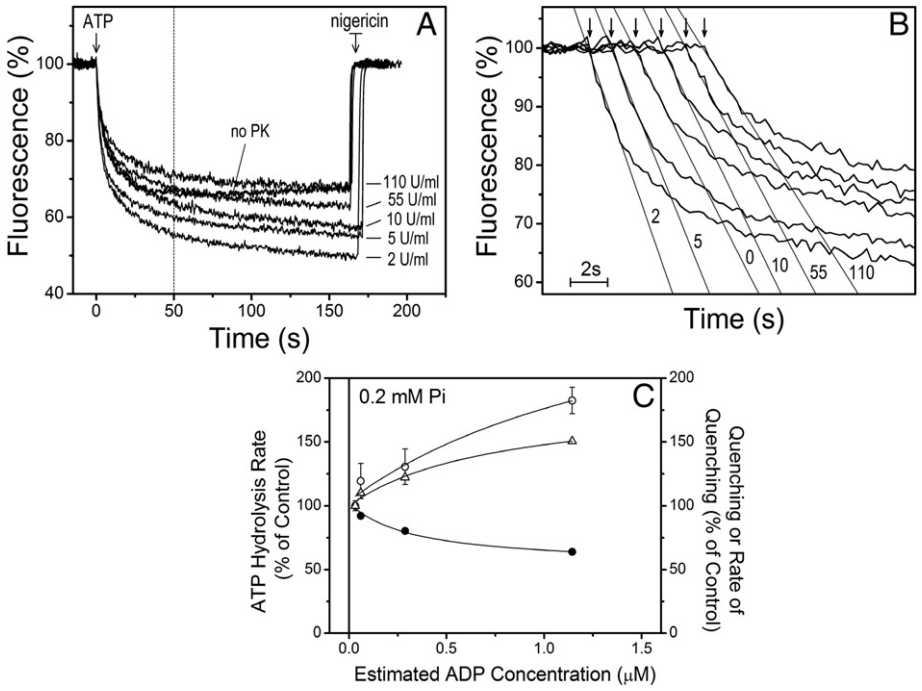

Fig. 5. ACMA fluorescence quenching at constant Pi concentration in the presence of increasing PK activity. (A) The ACMA assay was carried out as described in the legend of Fig. 2, but the reaction mixture contained in addition 200 μM Pi, 2 mM PEP and increasing activities of PK as indicated. The trace recorded in the absence of PK (thick line) can also be recognized by its slow recovery of fluorescence. (B) The traces from (A) are reported on a shorter time scale and displaced along the time axis for showing the initial rates of quenching. The arrows indicate the time points of ATP addition. The linear fits were calculated over 2 s of reaction (9 data points). (C) The steady state ADP concentration for each PK concentration was estimated as described in the text. The percentage values of the initial rates of fluorescence quenching (○) and the percentage values of fluorescence quenching at t=50 s (Δ) relative to controls, i.e. to the values obtained at the lowest estimated ADP concentration estimated in the presence of 110 U/ml of PK (5.0% · s^{-1} and 29.5%, respectively), were determined from (B) and (A), and the values of the initial rates of ATP hydrolysis (●) relative to control (5.0 nmol ATP · s^{-1} · mg $protein^{-1}$) were measured in an enzyme-coupled ATP regenerating system as described in the text. The errors of the initial rates of quenching are the errors associated with the first-order coefficient of the linear regression. The curves through the data points are the best fit to the data of a hyperbolic function.

contrast, while the hydrolysis rate kept increasing with the PK activity (Fig. 4), both the overall quenching signal and the initial quenching rate were markedly decreased (Fig. 5A, B). To check for possible interferences of the PK/PEP components with the permeability system of the membrane, the NADH-induced quenching was monitored in the presence of PEP and of increasing PK amounts, or the ATP-induced quenching was monitored in the presence of PEP alone or of PK alone or pyruvate. Again, no alteration of the quenching signal could be detected under these conditions, letting us conclude that the decrease in the quenching was due to a decrease of the proton translocation rate by the ATP synthase with increasing PK, in spite of the increasing rate of ATP hydrolysis.

The ADP concentrations present at the different PK activities can be calculated by imposing a steady state concentration for ADP, in which its rate of production by the ATP hydrolysis reaction ($v_{(hyd)}$) balances the rate of ADP depletion by the PK ($v_{(PK)}$). The attainment of a steady state [ADP] is consistent with the fact that, after an initial pre-steady state, the hydrolysis rate in the presence of the PK-LDH system is constant. Assuming a Michaelis–Menten kinetics of the PK reaction, one has:

$$v_{(hyd)} = v_{(PK)} = \frac{V_{max}^{ADP} \cdot [ADP]_{ss}}{[ADP]_{ss} + K_M^{ADP}} \quad (1)$$

where $[ADP]_{ss}$ is the ADP concentration in the steady state, and V_{max}^{ADP} and K_M^{ADP} refer to the PK reaction. V_{max}^{ADP} was measured directly (see Materials and methods), K_M^{ADP}=0.3 mM was taken from the literature [37] and $v_{(hyd)}$ are those reported in Fig. 4. While competition between ATP and ADP, and other possible kinetic alterations of the PK activity, have not been considered here, this calculation should provide a good first estimate of $[ADP]_{ss}$.

In Fig. 5C, the hydrolysis rates from Fig. 4 (closed circles) and the quenching data from Fig. 5A, B (open circles: quenching rates, triangles: quenching value at t=50 s) were plotted as a function of the calculated steady state ADP concentration. The lowest calculated ADP concentration corresponds to the highest PK activity (110 U/ml). In such a plot the diverging course between the ATP hydrolysis and the quenching data can be fully appreciated, as well as their dependency on the estimated ADP concentration. Noticeably, the very low ADP concentrations calculated in such a way (submicromolar range) indicate that a very high affinity binding site for ADP is involved.

3.5. Effect of ADP depletion on proton pumping as a function of Pi concentration

Similar experiments were performed at different concentrations of Pi and the final results are summarized in Fig. 6, where the quenching level at t=50 s (Fig. 6A) and the initial quenching rates (Fig. 6B) at different PK activities are plotted as a function of Pi. At all intermediate PK activities, a maximum of both quenching level and initial quenching rate was observed close to 100–200 μM Pi, followed by a decrease at higher concentrations. This biphasic course, as well as the extent of Pi inhibition in the high concentration range, were progressively attenuated at the highest PK activities, until no biphasicity was detectable at PK=110 U/ml, and a very weak inhibition was left. The biphasic trend observed at the intermediate PK activities was similar to what was found in the absence of PK (reported for comparison in Fig. 6A, B, open symbols) and was again particularly striking, given that the ATP hydrolysis rates were, on the contrary, monotonically decreasing as a function of Pi (see Fig. 4) at all the intermediate PK activities tested.

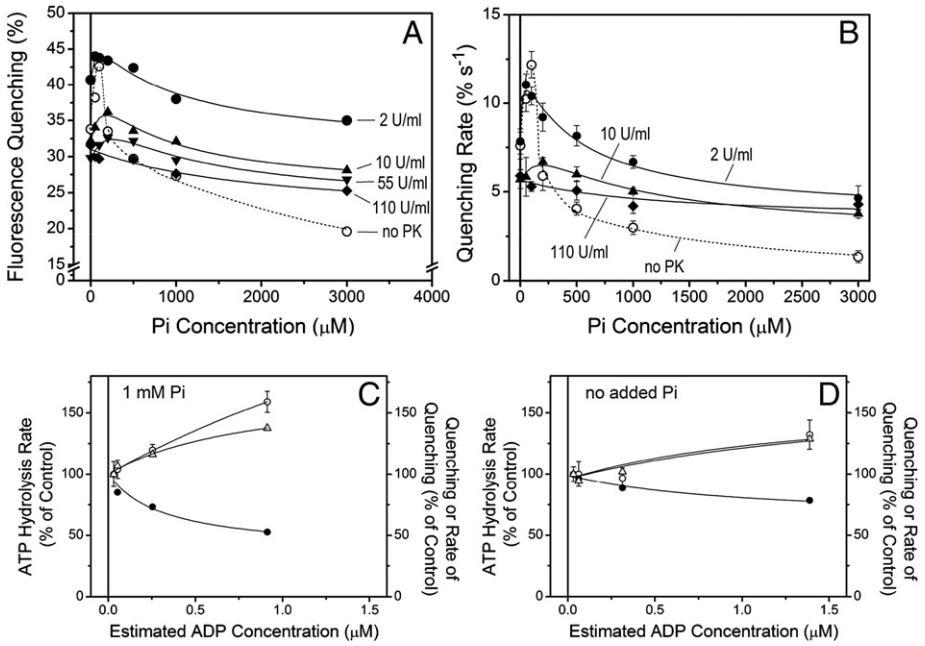

Fig. 6. ACMA fluorescence quenching as a function of Pi concentration in the presence of increasing PK activity. The ACMA assay was carried out as described in the legend of Fig. 2, but contained in addition 2 mM PEP and variable concentrations of PK and Pi as indicated. (A) The fluorescence quenching at t=50 s is plotted as a function of the added Pi concentration for each PK activity. The open symbols (no added PK) are reported from Fig. 2D for comparison. (B) The initial rates of fluorescence quenching were determined by the linear fits calculated over 1 s of reaction (5 data points) and are plotted as a function of the added Pi concentration for each indicated PK activity. The data at PK=55 U/ml were omitted for clarity. The errors of the initial rates of quenching are the errors associated with the first-order coefficient of the linear regression. The open symbols (no added PK) are reported from Fig. 2D for comparison. (C) The ADP concentration for each PK activity at 1 mM Pi was estimated as described in the text. The percentage values of the initial rates of fluorescence quenching (O) and the percentage values of fluorescence quenching at t=50 s (Δ) relative to controls, as specified in the legend of Fig. 5 (4.2% · s^{-1} and 27.6%, respectively), are from (B) and (A) (values at 1 mM Pi), and the rate values of ATP hydrolysis (●) relative to control (4.8 nmol ATP · s^{-1} · mg $protein^{-1}$) are from Fig. 4 (values at 1 mM Pi). The curves through the data points are the best fit to the data of a hyperbolic function. (D) The ADP concentration for each PK activity at no added Pi was estimated as described in the text. The percentage values of the initial rates of fluorescence quenching (O) and the percentage values of fluorescence quenching at t=50 s (Δ) relative to controls, as specified in the legend of Fig. 5 (5.9% · s^{-1} and 31.6%, respectively), are from (B) and (A) (values at 0 mM Pi), and the rate values of ATP hydrolysis (●) relative to control (4.9 nmol ATP · s^{-1} · mg $protein^{-1}$) are from Fig. 4 (values at 0 mM Pi). The curves through the data points are the best fit to the data of a hyperbolic function.

In addition, for all tested Pi concentrations, a trend similar to the one recorded at Pi=200 μM (Fig. 5) was evident: the lowest PK activity was the one at which both quenching level at t=50 s and initial quenching rate were the highest, and increasing PK activities induced a decrease of both these parameters. Also for these series of data, it was possible to calculate the steady state ADP concentration present in each assay and to plot the hydrolysis and quenching data as a function of $[ADP]_{ss}$ for each Pi concentration. In Fig. 6C one such plot is presented, in which the Pi concentration was 1 mM. In Fig. 6D the analogous plot is presented for the data obtained in the absence of added Pi; also in this latter case, the same divergent trend between hydrolysis and quenching is evident, as in the presence of Pi, indicating that ADP alone was also able to induce the phenomenon, although to a lower extent and with a lower binding affinity (the Pi present at the beginning of the reaction as a contaminant in the ATP solution was not higher than 0.5 μM, as measured by the green malachite method [24], and the Pi released during 50 s of ATP hydrolysis can be calculated and was not higher than 6 μM, i.e. negligibly small).

We conclude that the binding of ADP at very low concentration, and more markedly when Pi is present, induces in the ATP synthase a higher efficiency state, in which more protons per hydrolyzed ATP are translocated across the membrane.

4. Discussion

The major finding of the present work was that low concentrations of ADP and Pi inhibit the rate of ATP hydrolysis by the ATP synthase in *E. coli* internal membranes, while at the same time increase the rate of inward proton translocation. This experimental observation can be rationalized if it is assumed that, in binding these two ligands, the ATP synthase changes its catalytic mode, shifting from a partially uncoupled to a fully coupled ATP hydrolysis. This general conclusion parallels the one previously reached for the ATP synthase of *Rb. capsulatus* [22]. The occurrence of this phenomenon in these two Prokaryotes suggests that it might be a common feature in the prokaryotic ATP synthases, and possibly in the eukaryotic ones as well.

To our knowledge, a modulation of the coupling efficiency by physiological ligands has never been documented in any other ATP synthase so far, even though states of uncoupling have been reported in mutated, or chemically modified, ATP synthases [13–18], and in the presence of non-physiological ligands, such as Ca^{2+} and sulfite [19–21]. The results obtained in the laboratories of Capaldi [38] and Yoshida [39], according to which the trapping of the ε subunit in two different conformations generates either a "synthase" or a "hydrolase" form, can be considered consistent with the existence of two conformations having different coupling efficiencies, although alternative mechanisms could also explain those experimental findings. An intrinsic uncoupling has been reported for other chemiosmotic enzymes such as cytochrome oxidase (reviewed in [40]), V-ATPases [41–43], and Ca-ATPases (reviewed in [44]), in which its possible regulatory role has been discussed. Analogously, a regulatory role can also be hypothesized for the intrinsic uncoupling we observe in the ATP synthase, since it is possible that the intracellular Pi concentration varies in the hundreds of micromolar range. On the other hand, it seems likely that the protonmotive force also have a role in modulating the pump efficiency, and the binding competition with ATP as well, even though these possibilities have not been explored in the present work.

Similarly as seen in the ATP synthase of *Rb. capsulatus*, the ADP concentrations able to induce this phenomenon were in the sub-micromolar range, and could be attained during hydrolysis only by supplementing the assays with an ATP regenerating system acting as

an ADP trap. This implies the involvement of a site for ADP binding, whose very high affinity, manifest even in the presence of a large excess of ATP, is a strong indication in favor of its catalytic nature. The presence on the enzyme of such a site is consistent with measurements performed, in the absence of a proton gradient, in an *E. coli* ATP synthase in which Trp's introduced through mutagenesis into the catalytic sites were used as fluorescence reporters of nucleotide binding; these measurements detected two ADP binding sites with Kd of 0.18 and 13 μM respectively [45]. Very recently, ADP trapping with an ATP regenerating system has revealed also in the ATP synthase of *P. denitrificans* a high affinity ADP binding site, whose occupancy was required for maintaining the activated state of the enzyme [46].

The uncoupling/coupling transition observed in the present work was dependent on Pi as well, similarly again to what was shown in *Rb. capsulatus*. However, a striking difference was that Pi, which slightly activated the hydrolysis in the photosynthetic bacterium, was instead inhibitory for hydrolysis in the *E. coli* enzyme, which makes the stimulation of the proton translocation rate observed at Pi concentration up to 100 μM even more striking. The bell shaped dependence of proton transport on Pi concentration suggests that two Pi binding sites are involved, one with higher affinity, whose occupancy increases the pumping efficiency (leading to an overall higher rate of proton translocation in spite of the underlying inhibition) and a second one with lower affinity, causing inhibition of hydrolysis (reflected in the inhibition of proton translocation visible at higher Pi concentrations). The apparent Kd measured for Pi inhibition of ATP hydrolysis was 140 μM (Fig. 1), while the steep rise of the ACMA quenching rate and steady state between 0 and 100 μM Pi (Fig. 2) indicates that the Kd for the high affinity site could be in the order of tens of μM. The effect on the hydrolysis rate of the higher affinity binding site cannot be determined from our results, since the experimental data as a function of Pi could be fitted not only by a single hyperbolic function but equally well by the sum of two hyperbolic functions with two Kd's, one higher and one lower than 140 μM. The occurrence of two Pi binding sites has been shown in the isolated EF_1 by direct binding studies, and the resulting Kd (at pH 7.5) were both in the range of 0.1 mM [47]. In addition, Pi binding to EF_1 has been demonstrated indirectly through its effect on the trypsinization pattern of the ε subunit (apparent Kd=50 μM) [48], and its binding to EF_1 and EF_1F_O through the changes induced in the emission intensity of a fluorescent probe covalently bound to the γ subunit (apparent Kd=280 μM) [30]. An inhibition of ATP hydrolysis by Pi has also been reported, under deenergized conditions, in the isolated and reconstituted EF_1F_O (apparent Kd=500 μM) [23], and in the isolated EF_1 (apparent Kd=280 μM) [30]. In the light of the present data (Fig. 4), it should be considered that the value of the apparent Kd can depend on the fraction of ATP synthase molecules which have ADP bound. Moreover, according to data obtained in chloroplasts [49] and in *P. denitrificans* [50], the ATP synthase affinity for Pi may depend on the extent of the protonmotive force.

Both the Pi-inhibition of hydrolysis and the Pi-induced enhancement of coupling efficiency were lost in our system when the ADP concentration was drastically lowered by the presence of high amounts of the ADP-trapping PK (Figs. 4 and 6), indicating that these Pi effects were strictly dependent on the occupancy of a very high affinity binding site for ADP. The ADP requirement for the Pi-inhibition of hydrolysis is in agreement with the results obtained in the isolated and reconstituted EF_1F_O [23]. Interestingly, the presence of Pi has also been shown to be required for relief of ADP inhibition by the protonmotive force in TF_1F_O, both in the wild-type and in a mutant lacking the C-terminal domain of the ε subunit [51]. Similarly, data obtained in the bovine mitochondrial F_1 [52] showed that the preliminary incubation of ADP at concentrations equimolar with F_1 (μM range) was necessary for F_1 to bind Pi (present at 500 μM); this high affinity ADP binding site was also shown by the same group to be exchangeable and catalytic [53]. The most straightforward picture is that a catalytic site binds ADP, thereby closing the β subunit, and creating after this closure a Pi binding site which reinforces the closure.

In summary, the data presented in this work indicate that Pi can modulate the coupling efficiency of EF_1F_O, by binding to a high affinity site filled with ADP. We think that this modulation is likely to be brought about by the interconversion of two states of the enzyme, one of which has a lower coupling efficiency than the other. The possibility of modulating the coupling efficiency might require the existence of a structural device acting somehow as a clutch. The ε subunit appears to us as a possible candidate for this role, since it has frequently been indicated as a key regulatory and structural feature in the coupling mechanism (see e.g. [13–18,54] and for reviews [55–58]). In particular, the drastic changes in the ε trypsinization pattern induced by Pi [48] are consistent with Pi triggering the interconversion between two conformations, and the occurrence of drastically different conformations in this subunit has been confirmed by structural [59,60] and mutational studies [38,39]. One of these different conformations of the ε subunit could induce a more frequent slippage for instance within the rotor at the joint between the γ subunit and the c-subunit ring, or between stator and rotor at the interface $\alpha_3\beta_3$-barrel/γ-shaft. This last possibility would be consistent with the finding that mechanically driven ATP synthesis in TF_1 was more efficient if the ε subunit was added [61]. Interestingly, the ε subunit appears to control the conformations of the γ subunit (reviewed in [56]) and to modulate the rate of Pi release under unisite conditions [62].

An alternative possibility is that the observed uncoupling phenomena could be related to a premature release of the hydrolysis products from a catalytic site perturbing the ordered release sequence necessary for a productive cooperative interaction within the $\alpha_3\beta_3$ hexamer. The analysis of such an interpretation would require a careful correlation between a kinetic reaction model, the rotational mechanism and the energetics of the different catalytic sites (for this type of analysis see in particular [63,64]).

A final consideration is that, if indeed the switching from a low to a high efficiency state of the enzyme is brought about by ADP and Pi binding to a high affinity catalytic site, this binding has to be transient, otherwise there would be no chance of observing a more coupled hydrolysis. In other words, the ligands have to dissociate from the enzyme in steps subsequent to the binding and to the conformational switch. The two ligands could be released as such, or even as ATP, if a sufficiently high protonmotive force is available. As already noted [22], it is interesting in this respect that low levels of ATP synthesis, from medium ADP and Pi, are always found during ATP hydrolysis in the presence of a protonmotive force (so called "ATP-Pi exchange") even at very high ATP/ADP ratios [65,66]. Moreover, single molecule experiments have shown that the MgADP-inhibited TF_1F_O could be reactivated by a forced rotation of the γ subunit not only in the hydrolysis but also in the synthesis direction [67], which suggests that F_1F_O can release tightly bound ADP either as such or, possibly, as ATP.

Acknowledgements

We thank Dr. Stan Dunn for insightful discussions. This work has been supported by the grant PRIN Project number 2005052128_004 from the Italian Ministery for Education of University and Research (MIUR).

References

[1] P.D. Boyer, The ATP synthase—a splendid molecular machine, Annu. Rev. Biochem. 66 (1997) 717–749.
[2] R.H. Fillingame, W. Jiang, O.Y. Dmitriev, Coupling H^+ transport to rotary catalysis in F-type ATP synthases: structure and organization of the transmembrane rotary motor, J. Exp. Biol. 203 (2000) 9–17.
[3] M. Yoshida, E. Muneyuki, T. Hisabori, ATP synthase—a marvellous rotary engine of the cell, Nat. Rev., Mol. Cell Biol. 2 (2001) 669–677.

[4] R.A. Capaldi, R. Aggeler, Mechanism of the F(1)F(0)-type ATP synthase, a biological rotary motor, Trends Biochem. Sci. 27 (2002) 154–160.
[5] S. Wilkens, Rotary molecular motors, Adv. Protein Chem. 71 (2005) 345–382.
[6] J.P. Abrahams, A.G. Leslie, R. Lutter, J.E. Walker, Structure at 2.8 Å resolution of F1-ATPase from bovine heart mitochondria, Nature 370 (1994) 621–628.
[7] P.D. Boyer, W.E. Kohlbrenner, The present status of the binding-change mechanism and its relation to ATP formation by chloroplasts, in: B.R. Selman, S. Selman-Reimer (Eds.), Energy Coupling in Photosynthesis, Elsevier North Holland, New York, 1981, pp. 231–240.
[8] P.D. Boyer, The binding change mechanism for ATP synthase—some probabilities and possibilities, Biochim. Biophys. Acta 1140 (1993) 215–250.
[9] K. Kinosita Jr., K. Adachi, H. Itoh, Rotation of F1-ATPase: how an ATP-driven molecular machine may work, Annu. Rev. Biophys. Biomol. Struct. 33 (2004) 245–268.
[10] H.S. Van Walraven, M.J. Scholts, H. Lill, H.C. Matthijs, R.A. Dilley, R. Kraayenhof, Introduction of a carboxyl group in the loop of the F0 c-subunit affects the H+/ATP coupling ratio of the ATP synthase from Synechocystis 6803, J. Bioenerg. Biomembr. 34 (2002) 445–454.
[11] R.A. Schemidt, J. Qu, J.R. Williams, W.S. Brusilow, Effects of carbon source on expression of F0 genes and on the stoichiometry of the c subunit in the F1F0 ATPase of *Escherichia coli*, J. Bacteriol. 180 (1998) 3205–3208.
[12] K. Olsson, S. Keis, H.W. Morgan, P. Dimroth, G.M. Cook, Bioenergetic properties of the thermoalkaliphilic *Bacillus* sp. strain TA2.A1, J. Bacteriol. 185 (2003) 461–465.
[13] Y. Zhang, R.H. Fillingame, Subunits coupling H+ transport and ATP synthesis in the *Escherichia coli*–cys cross-linking of F1 subunit epsilon to the polar loop of F0 subunit c, J. Biol. Chem. 270 (1995) 24609–24614.
[14] R. Aggeler, F. Weinreich, R.A. Capaldi, Arrangement of the epsilon subunit in the *Escherichia coli* ATP synthase from the reactivity of cysteine residues introduced at different positions in this subunit, Biochim. Biophys. Acta 1230 (1995) 62–68.
[15] J.L. Gardner, B.D. Cain, Amino acid substitutions in the a subunit affect the epsilon subunit of F1F0 ATP synthase from *Escherichia coli*, Arch. Biochem. Biophys. 361 (1999) 302–308.
[16] Y.B. Peskova, R.K. Nakamoto, Catalytic control and coupling efficiency of the *Escherichia coli* FoF1 ATP synthase: influence of the Fo sector and epsilon subunit on the catalytic transition state, Biochemistry 39 (2000) 11830–11836.
[17] D.J. Cipriano, Y. Bi, S.D. Dunn, Genetic fusions of globular proteins to the epsilon subunit of the *Escherichia coli* ATP synthase: implications for in vivo rotational catalysis and epsilon subunit function, J. Biol. Chem. 277 (2002) 16782–16790.
[18] D.J. Cipriano, S.D. Dunn, The role of the epsilon subunit in the *Escherichia coli* ATP synthase. The C-terminal domain is required for efficient energy coupling, J. Biol. Chem. 281 (2006) 501–507.
[19] U. Pick, M. Weiss, A light-dependent dicyclohexylcarbodiimide-sensitive Ca-ATPase activity in chloroplasts which is not coupled to proton translocation, Eur. J. Biochem. 173 (1988) 623–628.
[20] R. Casadio, B.A. Melandri, CaATP inhibition of the MgATP-dependent proton pump (H+-ATPase) in bacterial photosynthetic membranes with a mechanism of alternate substrate inhibition, J. Bioinorg. Chem. 1 (1996) 284–291.
[21] P. Cappellini, P. Turina, V. Fregni, B.A. Melandri, Sulfite stimulates the ATP hydrolysis activity of but not proton translocation by the ATP synthase of *Rhodobacter capsulatus* and interferes with its activation by delta muH+, Eur. J. Biochem. 248 (1997) 496–506.
[22] P. Turina, D. Giovannini, F. Gubellini, B.A. Melandri, Physiological ligands ADP and Pi modulate the degree of intrinsic coupling in the ATP synthase of the photosynthetic bacterium *Rhodobacter capsulatus*, Biochemistry 43 (2004) 11126–11134.
[23] S. Fischer, P. Gräber, P. Turina, The activity of the ATP synthase from *Escherichia coli* is regulated by the transmembrane proton motive force, J. Biol. Chem. 275 (2000) 30157–30162.
[24] P. Turina, A. Rebecchi, M. D'Alessandro, S. Anefors, B.A. Melandri, Modulation of proton pumping efficiency in bacterial ATP synthases, Biochim. Biophys. Acta 1757 (2006) 320–325.
[25] M.E. Mosher, L.K. White, J. Hermolin, R.H. Fillingame, H+-ATPase of *Escherichia coli*. An uncE mutation impairing coupling between F1 and Fo but not Fo-mediated H+ translocation, J. Biol. Chem. 260 (1985) 4807–4814.
[26] M.M. Bradford, A rapid and sensitive method for the quantitation of microgram quantities of protein utilizing the principle of protein–dye binding, Anal. Biochem. 72 (1976) 248–254.
[27] M. Nishimura, T. Ito, B. Chance, Studies on bacterial photophosphorylation. III. A sensitive and rapid method of determination of photophosphorylation, Biochim. Biophys. Acta 59 (1962) 177–182.
[28] P.A. Lanzetta, L.J. Alvarez, P.S. Reinach, O.A. Candia, An improved assay for nanomole amounts of inorganic phosphate, Anal. Biochem. 100 (1979) 95–97.
[29] E. Muneyuki, M. Yoshida, D.A. Bullough, W.S. Allison, Heterogeneous hydrolysis of substoichiometric ATP by the F1-ATPase from *Escherichia coli*, Biochim. Biophys. Acta 1058 (1991) 304–311.
[30] P. Turina, Structural changes during ATP hydrolysis activity of the ATP synthase from *Escherichia coli* as revealed by fluorescent probes, J. Bioenerg. Biomembr. 32 (2000) 373–381.
[31] S. Schuldiner, H. Rottenberg, M. Avron, Determination of pH in chloroplasts. 2. Fluorescent amines as a probe for the determination of pH in chloroplasts, Eur. J. Biochem. 25 (1972) 64–70.
[32] R. Casadio, Measurements of transmembrane pH differences of low extents in bacterial chromatophores, Eur. Biophys. J. 19 (1991) 189–201.
[33] R. Casadio, S. Di Bernardo, P. Fariselli, B.A. Melandri, Characterization of 9-aminoacridine interaction with chromatophore membranes and modelling of the probe response to artificially induced transmembrane delta pH values, Biochim. Biophys. Acta 1237 (1995) 23–30.
[34] R. Casadio, B.A. Melandri, Calibration of the response of 9-amino acridine fluorescence to transmembrane pH differences in bacterial chromatophores, Arch. Biochem. Biophys. 238 (1985) 219–228.
[35] S. Löbau, J. Weber, A.E. Senior, Catalytic site nucleotide binding and hydrolysis in F1F0-ATP synthase, Biochemistry 37 (1998) 10846–10853.
[36] M.P. Turina, G. Venturoli, B.A. Melandri, Evaluation of the buffer capacity and permeability constant for protons in chromatophores from *Rhodobacter capsulatus*, Eur. J. Biochem. 192 (1990) 39–47.
[37] J.T. Mcquate, M.F. Utter, Equilibrium and kinetic studies of the pyruvic kinase reaction, J. Biol. Chem. 234 (1959) 2151–2157.
[38] S.P. Tsunoda, A.J. Rodgers, R. Aggeler, M.C. Wilce, M. Yoshida, R.A. Capaldi, Large conformational changes of the epsilon subunit in the bacterial F1F0 ATP synthase provide a ratchet action to regulate this rotary motor enzyme, Proc. Natl. Acad. Sci. 98 (2001) 6560–6564.
[39] T. Suzuki, T. Murakami, R. Iino, J. Suzuki, S. Ono, Y. Shirakihara, M. Yoshida, F0F1-ATPase/synthase is geared to the synthesis mode by conformational rearrangement of epsilon subunit in response to proton motive force and ADP/ATP balance, J. Biol. Chem. 278 (2003) 46840–46846.
[40] B. Kadenbach, Intrinsic and extrinsic uncoupling of oxidative phosphorylation, Biochim. Biophys. Acta 1604 (2003) 77–94.
[41] Y. Moriyama, N. Nelson, The vacuolar H+-ATPase, a proton pump controlled by a slip, Prog. Clin. Biol. Res. 273 (1988) 387–394.
[42] J.M. Davies, I. Hunt, D. Sanders, Vacuolar H(+)-pumping ATPase variable transport coupling ratio controlled by pH, Proc. Natl. Acad. Sci. 91 (1994) 8547–8551.
[43] M.L. Müller, M. Jensen, L. Taiz, The vacuolar H+-ATPase of lemon fruits is regulated by variable H^+/ATP coupling and slip, J. Biol. Chem. 274 (1999) 10706–10716.
[44] M.C. Berman, Slippage and uncoupling in P-type cation pumps; implications for energy transduction mechanisms and regulation of metabolism, Biochim. Biophys. Acta 1513 (2001) 95–121.
[45] S. Löbau, J. Weber, A.E. Senior, Catalytic site nucleotide binding and hydrolysis in F1F0-ATP synthase, Biochemistry 37 (1998) 10846–10853.
[46] T.V. Zharova, A.D. Vinogradov, Requirement of medium ADP for the steady-state hydrolysis of ATP by the proton-translocating *Paracoccus denitrificans* Fo.F1-ATP synthase, Biochim. Biophys. Acta 1757 (2006) 304–310.
[47] H.S. Penefsky, Pi binding by the F1-ATPase of beef heart mitochondria and of the *Escherichia coli* plasma membrane, FEBS Lett. 579 (2005) 2250–2252.
[48] J. Mendel-Hartvig, R.A. Capaldi, Catalytic site nucleotide and inorganic phosphate dependence of the conformation of the epsilon subunit in *Escherichia coli* adenosinetriphosphatase, Biochemistry 30 (1991) 1278–1284.
[49] V. Shoshan, H. Strotmann, The effect of phosphate on light-induced exchange of ADP at the tight nucleotide binding site of CF1, J. Biol. Chem. 255 (1980) 996–999.
[50] T.V. Zharova, A.D. Vinogradov, Energy-linked binding of Pi is required for continuous steady-state proton-translocating ATP hydrolysis catalyzed by F0.F1 ATP synthase, Biochemistry 45 (2006) 14552–14558.
[51] B.A. Feniouk, T. Suzuki, M. Yoshida, Regulatory interplay between proton motive force, ADP, phosphate, and subunit epsilon in bacterial ATP synthase, J. Biol. Chem. 282 (2007) 764–772.
[52] I.A. Kozlov, E.N. Vulfson, Tightly bound nucleotides affect phosphate binding to mitochondrial F1-ATPase, FEBS Lett. 182 (1985) 425–428.
[53] I.Y. Drobinskaya, I.A. Kozlov, M.B. Murataliev, E.N. Vulfson, Tightly bound adenosine diphosphate, which inhibits the activity of mitochondrial F1-ATPase, is located at the catalytic site of the enzyme, FEBS Lett. 182 (1985) 419–424.
[54] S. Duvezin-Caubet, M. Caron, M.F. Giraud, J. Velours, J.P. di Rago, The two rotor components of yeast mitochondrial ATP synthase are mechanically coupled by subunit delta, Proc. Natl. Acad. Sci. U. S. A. 100 (2003) 13235–13240.
[55] S.D. Dunn, A barrel in the stalk, Nat. Struct. Biol. 2 (1995) 915–918.
[56] R.A. Capaldi, B. Schulenberg, The epsilon subunit of bacterial and chloroplast F(1)F(0) ATPases. Structure, arrangement, and role of the epsilon subunit in energy coupling within the complex, Biochim. Biophys. Acta 1458 (2000) 263–269.
[57] Y. Evron, E.A. Johnson, R.E. McCarty, Regulation of proton flow and ATP synthesis in chloroplasts, J. Bioenerg. Biomembr. 32 (2000) 501–506.
[58] B.A. Feniouk, T. Suzuki, M. Yoshida, The role of subunit epsilon in the catalysis and regulation of FOF1-ATP synthase, Biochim. Biophys. Acta 1757 (2006) 326–338.
[59] C. Gibbons, M.G. Montgomery, A.G. Leslie, J.E. Walker, The structure of the central stalk in bovine F(1)-ATPase at 2.4 A resolution, Nat. Struct. Biol. 7 (2000) 1055–1061.
[60] A.J. Rodgers, M.C. Wilce, Structure of the gamma–epsilon complex of ATP synthase, Nat. Struct. Biol. 11 (2000) 1051–1054.
[61] Y. Rondelez, G. Tresset, T. Nakashima, Y. Kato-Yamada, H. Fujita, S. Takeuchi, H. Noji, Highly coupled ATP synthesis by F1-ATPase single molecules, Nature 433 (2005) 773–777.
[62] S.D. Dunn, V.D. Zadorozny, R.G. Tozer, L.E. Orr, Epsilon subunit of *Escherichia coli* F1-ATPase: effects on affinity for aurovertin and inhibition of product release in unisite ATP hydrolysis, Biochemistry 26 (1987) 4488–4493.

[63] K. Kinosita Jr., K. Adachi, H. Itoh, Rotation of F1-ATPase: how an ATP-driven molecular machine may work, Annu. Rev. Biophys. Biomol. Struct. 33 (2004) 245–268.
[64] Y.Q. Gao, W. Yang, M. Karplus, A structure-based model for the synthesis and hydrolysis of ATP by F1-ATPase, Cell 123 (2005) 195–205.
[65] A. Baccarini-Melandri, B.A. Melandri, Partial resolution of phosphorylating system of *Rps. capsulata*, Methods Enzymol. 23 (1971) 556–561.
[66] J.W. Davenport, R.E. McCarty, Quantitative aspects of adenosine triphosphate-driven proton translocation in spinach chloroplast thylakoids, J. Biol. Chem. 256 (1981) 8947–8954.
[67] Y. Hirono-Hara, K. Ishizuka, K. Kinosita Jr., M. Yoshida, H. Noji, Activation of pausing F1 motor by external force, Proc. Natl. Acad. Sci. U. S. A. 102 (2005) 4288–42893.